Evidence of extensive lunar crust formation in impact melt sheets 4,330 Myr ago

Journal Item

Evidence of extensive lunar crust formation in impact melt sheets 4330 Myr ago

White, L. F[1,2*], Černok, A[1,2,3], Darling, J. R[4], Whitehouse, M.J. [5], Joy, K. H.[6], Cayron, C[7], Dunlop, J[4], Tait, K. T[1,2] & Anand, M[3,8].

[1]*Centre of Applied Planetary Mineralogy, Department of Natural History, Royal Ontario Museum, Toronto, Ontario, M5S 2C6, Canada.*

[2]*Department of Earth Sciences, University of Toronto, Toronto, Ontario, M5S 3B1, Canada.*

[3]*School of Physical Sciences, The Open University, Milton Keynes, MK7 6AA, UK.*

[4]*School of Earth and Environmental Sciences, Burnaby Building, Burnaby Road, University of Portsmouth, Portsmouth, PO1 3QL, UK.*

[5]*Swedish Museum of Natural History, Box 50007, SE-104 05 Stockholm, Sweden*

[6]*School of Earth and Environmental Science, University of Manchester, Oxford Road, Manchester, M13 9PL, UK.*

[7]*Laboratory of ThermoMechanical Metallurgy (LMTM), École Polytechnique Fédérale de Lausanne (EPFL), Rue de la Maladière 71b,2000 Neuchâtel, Switzerland.*

[8]*Department of Earth Sciences, The Natural History Museum, Cromwell Road, London, SW7 5BD, UK.*

**Corresponding author: lwhite@rom.on.ca*

Accurately constraining the formation and evolution of the lunar magnesian (Mg) suite is key to understanding the earliest periods of magmatic crustal building that followed accretion and primordial differentiation of the Moon. However, the origin and evolution of these unique rocks is highly debated. Here, we report on the microstructural characterisation of a large (~250 μm) baddeleyite (monoclinic-ZrO_2) grain in Apollo troctolite 76535 that preserves quantifiable crystallographic relationships indicative of reversion from a precursor cubic-ZrO_2 phase. This observation places important constraints on the formation temperature of the grain (> 2300 °C) which endogenic processes alone fail to reconcile. We conclude that the troctolite crystallized directly from a large, differentiated impact melt sheet 4326 ± 14 million years (Myr) ago. These results suggest that impact bombardment would have played a critical role in the evolution of the earliest planetary crusts.

Insights into the formation, differentiation and impact bombardment of planetary bodies have been derived through geodynamic modelling, remote sensing observations, and isotopic analysis of planetary meteorites and returned samples. The resulting models are hindered by the paucity of mineralogical evidence that can place direct constraints on these very high temperature and pressure processes. Although many mineral thermobarometers can record geological temperatures ranging up to a maximum of ~1500 °C, empirical mineralogical and geochemical evidence of higher temperatures is often lost due to extensive

recrystallization and melting (and melt loss) at such conditions. Recently, microstructural analysis of the accessory mineral baddeleyite has revealed new insights into the high-temperature history of shock-melted rocks[1], with grains preserving microstructural evidence of high-temperature and high-pressure ZrO_2 polymorphs despite reversion to the stable monoclinic structure at ambient conditions. For example, tracing the phase heritage of baddeleyite disassociated from zircon to the cubic-ZrO_2 structure has constrained peak temperature conditions of a terrestrial impact melt to > 2370 °C at ambient surface pressures[1,2] (Figure 1), far in excess of that attainable with traditional mineral geothermometers[1]. Previous reports of cubic-ZrO_2 phase heritage are restricted to grains found in relatively young terrestrial rocks, such as ~37.8 Ma grains from the Mistastin Lake impact structure (Canada)[1,3]. As such, the ability for individual baddeleyite grains to preserve the rich microstructural heritage required to conduct phase reconstruction analysis across planetary timescales (over four billion years) is currently less established, though zirconia phase heritage has the potential to yield new insights into the high pressure and temperature history of Solar System processes[1,4]. Here, we undertake geochemical and microstructural analyses on an exceptional baddeleyite grain in a sample of the lunar Mg-suite, which reveals the diagnostic crystallographic relationships indicative of cubic-ZrO_2 phase heritage. This observation places new constraints on the mechanisms involved in lunar crustal evolution.

Lunar troctolite 76535, sampled by the Apollo 17 mission, is one of the most intensively studied samples from the Moon[5–7]. An unshocked, coarse-grained example of the Mg-suite, petrological observations suggest 76535 likely crystallized at a depth of 10 to 30 km within the lunar crust[8] before ejection and transportation to the Apollo sampling sites, potentially from as far afield as the South Pole Aitken basin[9]. This low-shock state is common among samples collected by the Apollo astronauts, with only ~1% of materials containing maskelynite, a diaplectic glass of feldspar composition only formed at high pressure (> 28 GPa)[10]. The rock has been considered chemically pristine (i.e. endogenously igneous) principally due to low abundances of highly siderophile elements[11], however Os-isotope ratios provide evidence for minor meteoritic contamination[12]. The Mg-suite as a whole preserves contradictory chemical signatures, with high Mg/(Mg+Fe) ratios, indicative of more primitive reservoirs, contrasting with high rare earth element signatures of their parent melts suggestive of an evolved magmatic source[6,13,14]. Reconciling these observations has proved challenging[15], and still represents a major area of uncertainty for lunar scientists that invokes a mantle overturn hypothesis[14]. The chronology of the studied sample has been

intensively investigated, yielding a ^{147}Sm-^{143}Nd age of 4307 ± 11 Myr[7], a Rb-Sr age of 4279 ± 52 Myr[7], and an ^{40}Ar-^{39}Ar age of 4249 ± 12 Myr[16], which collectively define a cooling rate of 3.9°C / Myr[7]. Following exhumation at 4249 Myr, as defined by the low temperature Ar-Ar chronometer, there is no evidence for further heating events above ~400 °C.

Within the analysed section (thin section ,51), a large (80 × 250 μm) subhedral baddeleyite crystal displays several distinctive crystallographic domains (each 2 to 50 μm in width) that are clearly observable at the resolution of optical microscopy (Figure 2a). No amorphous or crystalline silica (SiO_2) was observed in direct contact with the analysed baddeleyite grain, suggesting the phase does not represent a product of high-temperature dissociation from a zircon ($ZrSiO_4$) precursor[17] and instead remained pure ZrO_2 throughout its formation and evolution. Electron microprobe analysis (EMPA) of the grain reveals 1.26 wt% TiO_2 and 1.4 wt% HfO_2 (all EPMA data are reported in the supplementary materials), while other impurities (Mg, Ca, Fe, Al, and Si) constitute < 0.08 wt% each in total. Dating of the grain using secondary ion mass spectrometry (SIMS) reveals a spread of $^{207}Pb/^{206}Pb$ dates between 4334.5 ± 4.6 Myr (2σ uncertainty) and 4311.3 ± 6.7 Myr, yielding high scatter on the calculated weighted average age of 4326 ± 16 Ma (2 standard deviation uncertantity). The grain is between 40 and 63 million years older than previously reported ages from smaller baddeleyite grains within the same rock (4271 ± 29 Myr[5]). Detailed analysis of the grain using electron backscatter diffraction (EBSD) techniques facilitated the quantification of the variant orientations (Figure 2b), revealing a range of unique disorientation relationships between the domains: predominately 90°/<001>, 180°/<001>, and 180°/<9,0,10>. Reduction of the entire EBSD dataset using the ARPGE[18] software package highlights peaks in disorientation analysis at 90°, 120° and 180° which, along with the presence of three unique crystallographic axes in the <010> (*b*-axis) direction along three <100> cubic directions (Figure 2c), cannot be explained by reversion from the tetragonal or orthorhombic systems alone[1,2,4]. However, the phase heritage of the grain can be confidently associated with reversion from a single cubic-ZrO_2 precursor (Figure 2d).

Formative temperatures for cubic-ZrO_2 vary based on the major and trace element composition of the ZrO_2 grain. Although the influence of TiO_2 and HfO_2 on the P-T-t conditions required to induce high symmetary ZrO_2 polymorphs is unconstrained, oxide impurities typically have to occur in concentrations on the order of ~10 wt% to substantially influence phase transformation temperatures within the ZrO_2 system[19]. The temperature required to induce the cubic-ZrO_2 phase also varies based on the confining pressure of the

103 annealed sample[1], while the influence of oxygen fugacity on the transition is currently
104 unknown. However, at ~30 km depth (as estimated for the maximum formation depth of
105 76535[8]), an estimated ~0.2 GPa of confining pressure would facilitate formation of cubic-
106 ZrO_2 at ~2300 °C.
107 Thermal models of the Moon cannot reconcile these required temperatures through
108 endogenic processes alone[20], although impact-induced melting of crustal rocks has been
109 modelled to generate sufficient temperatures (~2300 °C) as to facilitate cubic-ZrO_2
110 formation[1]. While this previous occurrence of cubic phase heritage is reported from within
111 impact melt generated by a small (28 km) impact structure (Mistatin Lake), it is reasonable to
112 assume that larger melt sheets would reach comparable temperature conditions. Large impact
113 melt sheets are widely reported from the Moon, with recent studies into the formation of the
114 South Pole-Aitken basin suggesting that the impactor generated a 50 km deep melt pool[21]. An
115 event similar to this magnitude would be more than sufficient to produce the deep, super-
116 heated impact melt sheet required to produce both a coarse-grained assortment of
117 differentiated mafic rocks[22] and the high temperature cubic-ZrO_2 polymorph. It should be
118 noted that while sufficiently elevated temperatures would also be attained during the Moon-
119 forming impact itself[23], this event occurred up to 200 Myr ago, prior to the genesis of the
120 76535 troctolite[24]. In addition to these chronological constraints, modelling of the event
121 suggests ~100 % of the particles accreted into the lunar body would have reached
122 temperatures in excess of 5000°C[23]. Significantly in excess of the temperature required to
123 melt and vaporize ZrO_2[17], the Moon forming impact would lead to a complete loss of phase
124 heritage[1], and as such we move forward on the assumption that the Moon-forming impact
125 cannot have been responsible for the formation of the cubic ZrO_2 polymorph.
126 Although the crystallization potential of baddeleyite is directly controlled by the
127 oxygen fugacity and Zr content of the parent magma, in all scenarios it is one of the last
128 phases to crystallize out of a melt[25]. Thus, it is unlikely that a super-heated impact melt sheet
129 would solidify cubic-ZrO_2 directly unless unrealistically oversaturated in Zr (notably, this has
130 not been reported from large terrestrial impacts). Baddeleyite crystallizing directly from a
131 cooling impact melt would be expected to form at lower temperatures (< 1000 °C) and, thus,
132 not contain the interlocking reversion structures indicative of high-temperature phase
133 heritage. This suggests that our analysed baddeleyite grain crystallized as *m*-ZrO_2 within a
134 primordially differentiated presusor material (likely KREEP enriched) prior to incorporation
135 into the impact melt, whereby the elevated magmatic temperatures induced transformation to

the *c*-ZrO_2 structure (>2300 °C; Figure 1). This observation does not contradict the potential overturn of a lunar magma ocean[14], which could also explain the incorporation of a KREEP-rich layer into the impact melt environment. Given that disturbance of the U-Pb isotope system within the baddeleyite grain likely occurred during both phase transition[26] and subsequent annealing[27] it is assumed that the oldest Pb-Pb age recorded by the grain (4334.1 ± 4.2 Ma) represents the age of reversion from the high-temperature cubic-ZrO_2 structure. The 34 million year spread of Pb-Pb ages (4299.5 ± 8.8 to 4334.1 ± 4.2 Ma) supports this observation (Figure 3), hinting at staggered resetting of the U-Pb systematics during incorporation into the impact melt sheet. Fresh baddeleyite growth likely occurred at 4271 ± 29 Ma (based on previous dating of significantly smaller baddeleyite[5]) during the final crystallization stages of troctolite 76535 as supported by the observed age overlap with whole rock Ar-Ar chronometry[16]. Importantly, our new Pb-Pb data are concordant with two impact grown zircons recovered from a breccia containing clasts of shocked Mg-suite norite and impact melt (Apollo 15 sample 15455) that record ages of 4332 ± 6 Ma and 4326 ± 10 Myr [28]. These zircon grains contain remnant baddeleyite cores, and are interpreted as recrystallizing and dissociating during an impact event (whereby the $ZrSiO_4$ grains separate to the constituent oxides ZrO_2 and SiO_2 above ~1650 °C[17]). Coupled with our new temporal and temperature constraints from coarse grained troctolite 76535, these observations provide an argument for the generation of a large, super-heated impact meltsheet at ~4330 Myr ago, for which the Mg-suite appears to retain robust crystallographic and isotopic evidence.

Our findings provide new insights into the potential formation mechanisms for the earliest secondary lunar crust. Measurement of ^{207}Pb-^{206}Pb ages of baddeleyite and zircon, along with refractory ^{147}Sm-^{143}Nd and ^{146}Sm-^{142}Nd isotope systematics suggest that the ferroan anorthosite (FAN) suite of rocks formed as young as 4360 ± 3 Ma[29], supporting either a young Moon (which is problematic given the oldest lunar zircon, dated at 4417 ± 6 Ma[30]) or formation of early lunar crust through non magma ocean processes. Here, the discovery of the high temperature (≥ 2300 °C) cubic-ZrO_2 polymorph in Apollo 17 trocolitite 76535 suggests that large differentiated impact melt sheets could provide a mechanism for crustal formation immediately after lunar magma ocean crystallization, either in conjuction with or instead of rejuvenated or serial endogenic magmatism. This discovery supports interpretations of the Sr and Nd isotope systematics of FAN sample 60025 and Mg-suite sample 76535 which imply that both the FAN and Mg-suite crystallised from magmatic reservoirs that became isolated almost immediately before the crystallization of the rocks[7].

Although these Sr and Nd isotope systematics could also be explained by minimal differentiation of the bulk Moon[7], variations in major and trace element composition of the Mg-suite rocks support rapid formation and isolation of source magmas. This rapid generation of distinct source magmas for the FAN and Mg-suite could be facilitated by impact bombardment, with insulated melt sheets encouraging the localised slow cooling and differentiation of Mg-suite rocks. Any siderophile element signature inherited from the meteoritic impactor could be diluted and heterogeneously distributed throughout the large impact melt sheet[31], and thus measured abundances would vary throughout the resultant lithologies. In addition, at least one large impact around 4330 Myr ago would account for the preponderance of Sm-Nd and Lu-Hf model ages around this time[32], as well as an observed peak in zircon U-Pb ages[28]. Super-heated impact-induced melt sheets provide an alternative and, based on our new crystallographic and chronological evidence, more likely explanation for this observed clustering of ages.

Though a differentiated impact-melt sheet origin was previously proposed for the Mg-suite troctolites in the early 1990's[33], this model has been generally disregarded by more recent studies[14]. However, our new temperature and temporal constraints strongly suggest that at least one key sample from the Mg-suite, which records contradictory chemical signatures of primitive and evolved sources that are challenging to reconcile with endogenic lunar processes alone[15], originated from a super-heated impact melt sheet which likely homogenised varying quantities of primordially differentiated crustal suites. Though the melt sheet would likely have undergone differentiation and fractional crystallization[34], the isotopic and elemental composition of this melt is largely dependent on that of the target lithologies[35], suggesting incorporation of an underlying urKREEP component into the melt source of troctolite 76535. Such interactions would produce the conflicting chemical signatures and variable compositions observed in other samples from the Mg-suite, whilst retaining the 'pristine' siderophile elemental signature ascribed to the suite[12]. Thus, we suggest that the impact-melt sheet hypothesis likely explains the origin of at least some members of the enigmatic Mg-suite. On a larger scale, our findings provide strong evidence for at least one, though potentially multiple, large-scale bombardment events in the early history of the Moon ($\geq$ 4330 Myr ago), suggesting that the evolution of evolved planetary crusts around this time is intrinsically linked to impact events. Given the timing of this bombardment, it is possible that early impacts into a differentiating Moon may have provided the melting and mixing required to initiate overturn of lunar magma ocean cumulates around 4350 Myr ago. Such

impacts would also satisfy previous predictions that ancient basaltic magmatism (recently dated to 4370 - 4340 Myr ago[36]) would be triggered by large basin forming events[37]. Such evidence has previously remained concealed in the lunar rock record.

Although this study represents the sole report of prior cubic-ZrO_2 within a lunar sample, the implications of this discovery for crustal formation on the Moon should re-invigorate detailed investigations of existing and future returned lunar samples. Meteoritic baddeleyite are often highly deformed, and as such the discrete crystallographic structures incorporated into this phase heritage approach could be partially overprinted during shock ejection from the lunar surface. As such, the preservation potential of these features in meteoritic samples is currently unknown. Our discovery of cubic-ZrO_2 phase heritage in ancient (~4330 million years old) baddeleyite grains pushes back the preservation age of these crystallographic structures by ~4300 million years[17], revealing the robustness of microstructural phase heritage across the timescales required to probe the early Solar System. This crystallography-driven approach can thus be applied to a wide range of baddeleyite-bearing planetary lithologies in an effort to improve our understanding of early, high-temperature Solar System processes by directly interpreting the rock record of these planet-shaping events.

Main References

1. Timms, N. E. *et al.* Cubic zirconia in >2370 °C impact melt records Earth's hottest crust. *Earth Planet. Sci. Lett.* **477,** 52–58 (2017).
2. Cayron, C., Douillard, T., Sibil, A., Fantozzi, G. & Sao-Jao, S. Reconstruction of the cubic and tetragonal oarent grains from electron backscatter diffraction maps of monoclinic zirconia. *J. Am. Ceram. Soc.* **93,** 2541–2544 (2010).
3. Sylvester, P., Crowley, J. & Schmitz, M. U-Pb zircon age of Mistastin Lake crater, Labrador, Canada - implications for high-precision dating of small impact melt sheets and the end Eocene extinction. in *Mineralogical Magazine* 2295 (2013).
4. White, L. F. *et al.* Baddeleyite as a widespread and sensitive indicator of meteorite bombardment in planetary crusts. *Geology* **46,** 719–722 (2018).
5. Hinthorne, J. R., Conrad, R. & Andersen, C. A. Lead-lead age and trace element abundances in lunar troctolite 76535. in *Lunar and Planetary Science Conference Proceedings.* (1975).
6. Elrado, S. M., McCubbin, F. M. & Shearer Jr, C. K. Chromite symplectite in Mg-suite troctolite 76535 as evidence for infiltration metasmoatism of a lunar layered intrusion.

Geochim. Cosmochim. Acta **87,** 154–177 (2012).

7. Borg, L. E., Connelly, J. N., Cassata, W. S., Gaffney, A. M. & Bizzarro, M. Chronological implications for slow cooling of troctolite 76535 and temporal relationships between the Mg-suite and the ferroan anorthosite suite. *Geochim. Cosmochim. Acta* **201,** 377–391 (2017).

8. Gooley, R., Brett, R., Warner, J. & Smyth, J. . A lunar rock of deep crustal origin: sample 76535. *Geochim. Cosmochim. Acta* **38,** 1329–1339 (1974).

9. Garrick-Bethell, I. *et al.* Troctolite 76535: A sample of the Moon's South Pole-Aitken basin? *Icarus* **338,** (2020).

10. Rubin, A. E. Maskelynite in asteroidal, lunar and planetary basaltic meteorites: An indicator of shock pressure during impact ejection from their parent bodies. *Icarus* **257,** 221–229 (2015).

11. Warren, P. H. A concise compilation of petrologic information on possibly pristine nonmare Moon rocks. *Am. Mineral.* **78,** 360–376 (1993).

12. Day, J. M. D., Walker, R. J., James, O. B. & Puchtel, I. S. Osmium isotope and highly siderophile element systematics of the lunar crust. *Earth Planet. Sci. Lett.* **289,** 595–605 (2010).

13. Elrado, S. M., Draper, D. S. & Shearer Jr, C. K. Lunar Magma Ocean crystallization revisited: Bulk composition, early cumulate mineralogy, and the source regions of the highlands Mg-suite. *Geochim. Cosmochim. Acta* **75,** 3024–3045 (2011).

14. Shearer, C. K., Elrado, S. M., Petro, N. E., Borg, L. E. & McCubbin, F. M. Origin of the lunar highlands Mg-Suite: An integrated petrology, geochemistry, chronology, and remote sensing perpective. *Am. Mineral.* **100,** 294–325 (2015).

15. Taylor, S. R., Norman, M. D. & Esat, T. M. The Mg-suite and the highland crust: An unsolved enigma. in *Proceedings of the Lunar and Planetary Science Conference Vol. 24* (1993).

16. Garrick-Bethell, I., Weiss, B. P., Shuster, D. L., Tikoo, S. M. & Tremblay, M. M. Further evidence for early lunar magnetism from troctolite 76535. *J. Geophys. Res. Planets* **121,** 1–18 (2016).

17. Timms, N. E. *et al.* A pressure-temperature phase diagram for zircon at extreme conditions. *Earth-Science Rev.* **165,** 185–202 (2017).

18. Cayron, C. ARPGE: a computer program to automatically reconstruct the parent grains from electron backscatter diffraction data. *J. Appl. Crystallogr.* **40,** 1183–1188 (2007).

19. Swab, J. *Role of Oxide Additives in Stabilizing Zirconia for Coating Applications*.

(2001).
20. Zhang, N., Parmentier, E. M. & Liang, Y. A 3-D numerical study of the thermal evolution of the Moon after cumulate mantle overturn: The importance of rheology and core solidification. *J. Geophys. Res. Planets* **118,** 1789–1804 (2013).
21. Hurwitz, D. M. & Kring, D. A. Differentiation of the South Pole-Aitken basin impact melt sheet: Implications for lunar exploration. *J. Geophys. Res. Planets* **119,** 1110–1133 (2014).
22. Latypov, R., Chistyakova, S., Grieve, R. & Huhma, H. Evidence for igneous differentiation in Sudbury Igneous Complex and impact-driven evolution. *Nat. Commun.* 1–13 (2019). doi:10.1038/s41467-019-08467-9
23. Canup, R. M. & Asphaug, E. Origin of the Moon in a giant impact near the end of the Earth's formation. *Nature* **412,** 708–712 (2001).
24. Jacobson, S. A. *et al.* Highly Siderophile Elements in the Earth's Mantle as a Clock for the Moon-forming Impact. *Nature* **508,** 84–87 (2014).
25. Herd, C. D. K. *et al.* in *Microstructural Geochronology: Planetary Records Down to Atom Scale* (eds. Moser, D. E., Corfu, F., Darling, J. R., Reddy, S. M. & Tait, K.) 137–165 (American Geophysical Union, 2018).
26. White, L. F. *et al.* Atomic scale age resolution of planetary events. *Nat. Commun.* (2017). doi:10.1038/ncomms15597
27. Darling, J. R. *et al.* Variable microstructural response of baddeleyite to shock metamorphism in young basaltic shergottite NWA 5298 and improved U–Pb dating of Solar System events. *Earth Planet. Sci. Lett.* **444,** 1–12 (2016).
28. Crow, C. A., McKeegan, K. D. & Moser, D. E. Coordinated U–Pb geochronology, trace element, Ti-in-zircon thermometry and microstructural analysis of Apollo zircons. *Geochim. Cosmochim. Acta* **202,** 264–284 (2017).
29. Borg, L. E., Connelly, J. N., Boyet, M. & Carlson, R. W. Chronological evidence that the Moon is either young or did not have a global magma ocean. *Nature* **477,** 70–72 (2011).
30. Nemchin, A. *et al.* Timing of crystallization of the lunar magma ocean constrained by the oldest zircon. *Nat. Geosci* **2,** 133–136 (2009).
31. Petrus, J. A., Ames, D. E. & Kamber, B. S. On the track of the elusive Sudbury impact: gepchemical evidence for a chondrite or comet bolide. *Terra Nov.* **27,** 9–20 (2015).
32. Borg, L. E., Gaffney, A. M. & Shearer, C. K. A review of lunar chronology revealing a

preponderance of 4.34-4.37 Ga ages. *Meteorit. Planet. Sci.* **50,** 715–732 (2015).
33. Hess, P. C. The petrogenesis of lunar troctolites. *J. Geophys. Res.* **99,** 19083–19093 (1994).
34. O'Connell-Cooper, C. D. & Spray, J. G. Geochemistry of the impact-generated melt sheet at Manicouagan: Evidence for fractional crystallization. *J. Geophys. Res. Solid Earth* **116,** B6 (2011).
35. Darling, K. R., Hawkesworth, C. J., Storey, C. D. & Lightfoot, P. C. Shallow impact: Isotopic insights into crustal contributions to the Sudbury impact melt sheet. *Geochim. Cosmochim. Acta* **74,** 5680–5696 (2010).
36. Snape, J. F. *et al.* Ancient volcanism on the Moon: Insights from Pb isotopes in the MIL 13317 and Kalahari 009 lunar meteorites. *Earth Planet. Sci. Lett.* **502,** 84–95 (2018).
37. Elkins-Tanton, L. T., Hager, B. H. & Grove, T. L. Magmatic effects of the lunar late heavy bombardment. *Earth Planet. Sci. Lett.* **222,** 17–27 (2004).
38. Park, J. *et al.* Newly determined Ar/Ar ages of lunar troctolite 76535. in *Proceedings of the 46th Lunar and Planetary Science Conference* (2015).
39. Heaman, L. M. & LeCheminant, A. N. Paragenesis and U-Pb systematics of baddeleyite (Zr02). *Chem. Geol.* **110,** 95–126 (1993).
40. Marchi, S. *et al.* High-velocity collisions from the lunar cataclysm recorded in asteroidal meteorites. *Nat. Geosci.* **6,** 303–307 (2013).
41. Hiesinger, H. *et al.* New crater counts of the South Pole-Aitken basin. in *EGU General Assembly* 8410 (2012).

Acknowledgments

L.F.W and A.C are funded by a Hatch postdoctoral fellowship. A.C. has received funding from the European Union's Horizon 2020 research and innovation programme under grant agreement No-704696 RESOLVE, and M.A's contribution to this work was partly funded by the UK Science and Technology Facilities Council (ST/L000776/1 & ST/P000657/1). The NordSIMS facility is supported by Swedish Research Council infrastructure grant no. 2017-00671 and the Swedish Museum of Natural History; this is NordSIMS publication no. 609. K.H.J acknowledges STFC grant ST/M001253 and Royal Society grant UF140190. J.R.D acknowledges STFC grant ST/S000291/1 and Royal Society Research Grant RG160237. We thank Geoff Long for conducting colloidal silica polishing of

the thin section to facilitate EBSD analysis of the target grain. M.A. thanks NASA CAPTEM for the allocation of polished thin section 76535,51.

Author Contributions

L.F.W., A.C., J.R.D. and M.A. designed the initial study. L.F.W., A.C., J.R.D. and J.D. conducted electron backscatter diffraction analysis of the baddeleyite grain. C.C. conducted phase reconstruction using the ARPGE and GenOVa software packages. A.C. and M.W conducted SIMS analysis on the baddeleyite grain. All authors discussed the results and interpretation, and commented on the manuscript at all stages.

Author Information

Reprints and permissions information is available at www.nature.com/reprints. The authors declare no competing financial interests. Readers are welcome to comment on the online version of the paper. Correspondence and requests for materials should be addressed to L.F.W (lwhite@rom.on.ca).

Competing Interests

The authors declare no competing interests.

Methods

All work was conducted *in situ* within a thin-section that was vibratory polished with 0.05 micron alumina. The target baddeleyite grain was located in section 76535,51 using traditional microscopy techniques, and backscatter electron (BSE) images were collected using a Zeiss EVO MA10 LaB_6 scanning electron microscope (SEM) housed at the University of Portsmouth. Micro- to nano-scale structural analysis was conducted by electron backscatter diffraction (EBSD) using an Oxford Instruments Nordlys EBSD detector mounted on the same SEM instrument. No coating was applied, and EBSD analyses were performed under variable pressure conditions, using N_2 to neutralize charging. The sample was tilted at 70° within the chamber at a working distance of 14 mm, before analysis using an electron beam with an accelerating voltage of 20 kV and a probe current of 1 nA. The grain was mapped using the AZTEC software package (Oxford instruments), which facilitates automated collection of kikuchi diffraction patterns from set spatial intervals. The grain was initially mapped at 1 μm step size to confirm the presence of complex microstructure

suggested by petrological imaging of the grain. To collect a more robust dataset, the grain was reanalyzed at 500 nm step size, to more fully capture smaller crystallographic domains. The complete map yielded 53,038 indexed baddeleyite data points. Monoclinic-ZrO_2 was indexed using ref [42], and although crystallographic cards for orthorhombic-ZrO_2, tetragonal-ZrO_2 and cubic-ZrO_2 were included during analysis the phases were never indexed by the software. Wild spike reduction was completed on all EBSD datasets, although no other form of raw data correction (i.e. infilling of zero solutions) was conducted.

Reconstruction of all indexed baddeleyite reveals a single cubic parent grain which can be attributed to the generation of all monoclinic orientations in the measured dataset (Supplementary Figure 1). Analysis of the entire EBSD dataset using the ARPGE[18] software package highlights peaks in disorientation analysis at 90°, 120° and 180° which can be associated with cubic to monoclinic reversion of the grain. These disorientations closely match those predicted by Type 2 orientation relationships (OR) ((100)m//(100)c & [010]m//[010]c)[2], matching those observed in impact melt samples at Mistastin Lake[1] (Supplementary Figure 2a). This observation is further strengthened by the presence of three unique crystallographic axes in the <010> (*b*-axis) direction along the three <100> cubic directions of the prior cubic grain, as shown by the stereographic pole figures of the <100>, <010> and <001> directions and their simulations made with the software GenOVa[43] in Supplementary Figure 2b,c which cannot be explained by reversion from the tetragonal or orthorhombic systems alone[2].

The pole figures of the planes are reported in Supplementary Figure 2b, whereby the comparison between the experimental and simulated pole figures also shows that Type 1 OR exists besides the major Type 2 OR. This additional OR explains the peaks at 80° and 115° in the disorientation histogram (Supplementary Figure 2a). To localize the intermediate tetragonal domains, the 12 monoclinic variants inherited from the cubic grains were partitioned into three packets of four variants sharing the same b-axis oriented along the same <100> *c*-axis (Supplementary Figure 2d). The analysis reveals that one b-packet dominates the two other ones, which proves that a majority (but not all) the baddeleyite grains come from a unique prior tetragonal domain (in blue in Supplementary Figure 2d) crossed by a second large tetragonal domain (in red) and smaller third domains (in green). Only a single, cubic parent can explain the microstructure observed here.

The thin-section was coated with ~30 nm layer of gold on the top of the carbon coat, to reduce gold accumulation in the cracks. Pb- isotopic measurements of baddeleyite were

performed using a CAMECA IMS1280 ion microprobe at the NordSIMS facility, Swedish Museum of Natural History (Stockholm), closely following previously reported protocols[36,44]. The Hyperion H201 RF plasma source was used to generate a 23kV impact energy, 2.5 nA, Gaussian focussed primary beam of O_2^- ions, which was used together with an in-run raster of 5 µm to yield a spot of ca 8 µm diameter. Oxygen flooding of the sample chamber was used to enhance secondary Pb ion yields from baddeleyite by a factor of 7. Secondary Pb^+ ions were mass filtered at M/ΔM of 4860 and detected simultaneously in four low-noise ion-counting electron multipliers. Detector gains were calibrated using BCR-2g basaltic glass and common Pb corrected $^{207}Pb/^{206}Pb$ ratios were further normalised to bracketing analyses (n = 6) of Phalaborwa baddeleyite (2060.6 Ma[45]). Data reduction was performed using an in-house developed software at NordSIMS. The $^{207}Pb/^{206}Pb$ ages assume the decay constants recommendations of Steiger and Jäger (1975) and are reported with 2σ errors. The effects of common lead on the measured $^{207}Pb/^{206}Pb$ ages were calculated using a variety of modelled scenarios, from terrestrial contamination to variable influence of lead from lunar basalt and KREEP terranes. In all cases, the measured age is only altered by < 0.8 Ma (Supplementary Table 4), minimising the risk of common lead resulting in the older than published values for baddeleyite in troctolite 76535.

Data Availability

The authors declare that data supporting the findings in this study are available within the paper and its Supplementary Information files. All other data are available from the corresponding author upon request.

Additional References

42. Smith, D. K. & Newkirk, W. The crystal structure of baddeleyite (monoclinic ZrO2) and its relation to the polymorphism of ZrO2. *Acta Crystallogr.* **18,** 983–991 (1965).
43. Cayron, C. GenOVa: a computer program to generate orientational variations. *J. Appl. Crystallogr.* **40,** 1179–1182 (2007).
44. Whitehouse, M. J., Kamber, D. S., Fedo, C. M. & Lepland, A. The importance of combined Pb and S isotope data from early Archaean rocks, southwest Greenland, for the interpretation of S-isotope signatures. *Chem. Geol.* **222,** 112–131 (2005).
45. Reischmann, T. Precise U/Pb age determination with baddeleyite (ZrO2), a case study from the Phalaborwa igenous complex, South Africa. *South African J. Geol.* **98,** 1–4 (1995).

Supplementary Information is available in the online version of the paper.

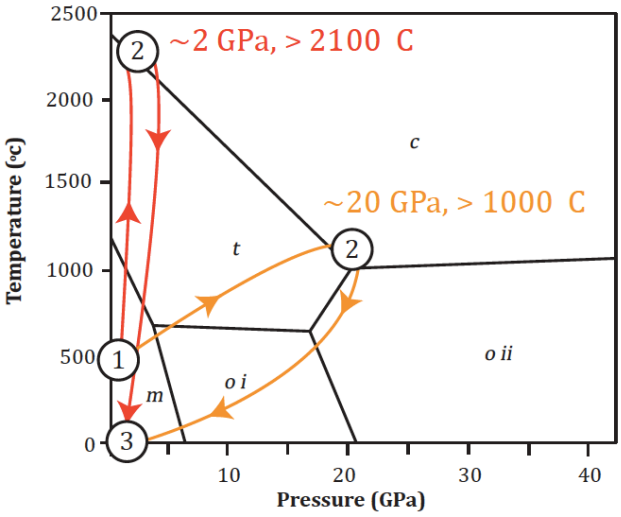

Figure 1: Phase diagram of the ZrO_2 system. Stable at ambient conditions, monoclinic-ZrO_2 (1) transitions to the meta-stable tetragonal-ZrO_2 (t) and cubic-ZrO_2 (c) structure at high temperature conditions (2) before reverting to m-ZrO_2 upon cooling (3). At high pressures, grains will transform through a series of orthorhombic-ZrO_2 polymorphs (o i and o ii). While the exact temperature required to induce the cubic structure varies based on confining pressure (e.g. red versus orange P-T pathways), if high pressure conditions were reached shock effects associated with > 20 GPa of loading would be observed in the troctolite. The pristine nature of troctrolite 76535 suggests no such shock pressures were experienced, supporting origin by a super-heated melt. This supports a formation temperature of at least 2300 °C for the cubic ZrO_2 structure, which cannot be attained by endogenic processes alone. (Adapted from ref [17]).

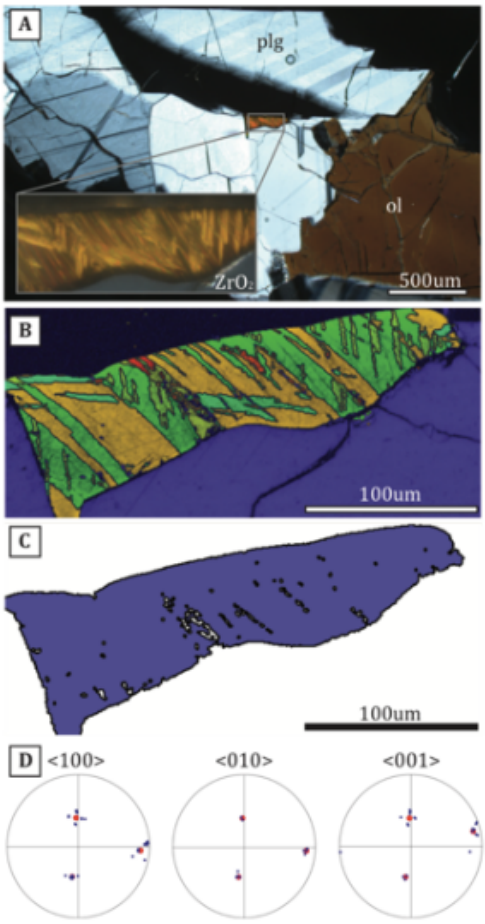

Figure 2: Optical imaging, EBSD data and parent grain reconstruction for the large baddeleyite grain in Apollo sample 76535. Cross polarized light (XPL) overview of the target grain, highlighting the crystalline and unshocked nature of the surrounding plagioclase (plg) and olivine (ol) (**A**). Inset image of target baddeleyite (ZrO_2) grain highlights the density and complexity of twin relationships observable even at low optical resolution (40x magnifcation). EBSD data reveal an abundance of monoclinic domains throughout the grain, with colour coded mapping of crystallographic orientations (enhanced from inverse pole figure) revealing structural complexity within the grain (**B**). Reconstruction of these measured domains using the ARPGE software package[18] is conducted by quantifying each monoclinic orientation before tracing relationships back to a single cubic precursor grain, as shown in (**C**). This process is aided by the disorientation relationships observed in <100>, <010> and <001> directional pole figures of the dataset (**D**), which reveal the correlation between measured baddeleyite orientations (blue data) and the calculated orientation of cubic precursors (red data). A small number of pixels could not be reconstructed in this manner, potentially representing neoblastic overgrowth during further annealing.

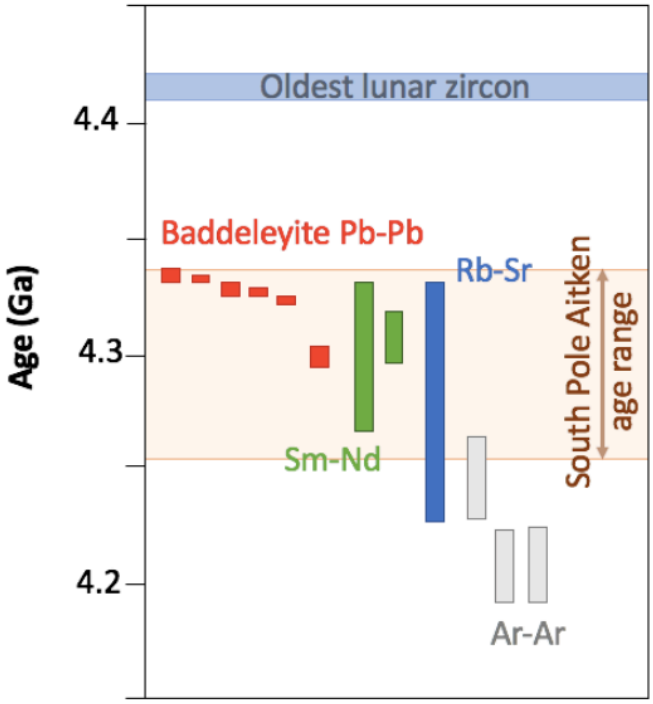

Figure 3: Pb-Pb data generated by SIMS analysis of the large reversion twinned baddeleyite grain in troctolite 76535, and comparison to published Sm-Nd[7], Rb-Sr[7] and Ar-Ar[38] chronology for the same rock. The mean squared weighted deviation of 13 suggests the ages record excess scatter, providing evidence that the spread of ages (between 4299.5 ± 4.4 Ma and 4334.1 ± 2.1 Ma) is real and not analytical. This partial age resetting on the grain scale is indicative of Pb loss induced during phase reversion, where the rapid heating and cooling associated with the impact melt sheet fail to completely homogenise the U-Pb systematics[26]. Importantly, our Pb isotope data define the age of Pb diffusion in baddeleyite (> 950 °C[39]), comparable to the previously described cooling rate[7]. Generated baddeleyite ages fall within previously defined age estimates for both the FAN and Mg suites of lunar rocks. For reference, ages of the oldest measured lunar zircon[30] and the estimated age of the South Pole Aitken basin[40,41], which has been modelled to be a potential source terrane[9], are also presented.